Port Everglades Flow Measurement System

Atlantic Oceanographic and Meteorological Laboratory
Miami, Florida

April 2013

Suggested Citation

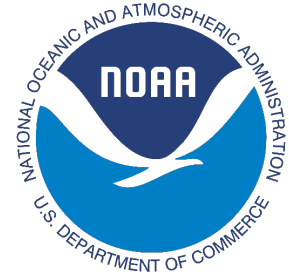## Acknowledgments

Disclaimer

Port Everglades Flow Measurement System

S. Jack Stamates[1]
Joseph R. Bishop[1]
Thomas P. Carsey[1]
Jules F. Craynock[1,2]
Michael L. Jankulak[1,3]
Charles A. Lauter[1,2]
Michael M. Shoemaker[1]

[1] NOAA-Atlantic Oceanographic and Meteorological Laboratory
Miami, Florida

[2] Retired from federal service

[3] University of Miami-Cooperative Institute for Marine and Atmospheric Studies
Miami, Florida

April 2013

Table of Contents

Acronyms

ADCP	Acoustic Doppler current profiler
AOML	Atlantic Oceanographic and Meteorological Laboratory
CTD	Conductivity-temperature-depth
FACE	Florida Area Coastal Environment
FIU	Florida International University
GPS	Global positioning system
H-ADCP	Horizontal acoustic Doppler current profiler
NDBC	National Data Buoy Center
NOAA	National Oceanic and Atmospheric Administration
PESC	Port Everglades shipping channel
SEFCRI	Southeast Florida Coral Reef Initiative
USCG	United States Coast Guard

Figures

Figures (continued)

Tables

Abstract

An acoustic Doppler current profiler was installed on the south side of the Port Everglades Inlet to measure the velocity of the water flow at levels starting near the surface and reaching down to near the channel bottom. The system was built using a commercial, horizontal-looking ADCP deployed in a hybrid manner to measure the vertical velocity structure. This system was calibrated so that its velocity measurements could estimate the mean channel velocity at specific depth layers by repeatedly transecting a vessel-mounted, down-looking ADCP across the channel at the location of the fixed system. The channel cross-sectional area at the location of the fixed system was measured, and a pressure sensor on the fixed system allowed the cross section of the channel to be estimated at the time of each velocity measurement. From the area and mean channel velocity measurements, an estimate of the volume transport per unit of time (Q) in a surface and deep layer was made. By integrating the Q measurements over a tidal phase, measurements of total volume transport per tidal phase in the surface and bottom layers were made. These volume estimates will be used to estimate the total seaward flux of certain substances measured by the Florida International University group during the study. Using an independent data set, the dispersion of materials advected seaward from the inlet into the coastal ocean was estimated.

1. Introduction

The Port Everglades Shipping Channel (PESC), located in Ft. Lauderdale, Florida (Figure 1), is one of the largest and busiest coastal inlets on the eastern coast of Florida (http://www.porteverglades.net/about-us/). The PESC serves as the entrance to Port Everglades harbor and is used by commercial shipping vessels, cruise ships, and recreational vessels. The PESC is 241 m wide at the location where the study system was deployed and has a maximum depth of 15 m. Inside the Port Everglades basin, waters from inland canals and surface runoff from metropolitan Broward County merge with oceanic waters and, twice a day on the ebb tide, some combination of these two water masses is transported seaward out of the PESC. Along the south Florida coast, there are three tracts of reefs that run parallel to the shore (Banks *et al.*, 2007). Anthropogenic nutrients and microbes contained in the waters exiting the PESC have the potential to impact these reefs and other coastal amenities.

As part of the Southeast Florida Coral Reef Initiative (SEFCRI, http://www.dep.state.fl.us/coastal/programs/coral/sefcri.htm), a project was proposed to study the Port Everglades Inlet by attempting to quantify the concentrations and fate of anthropogenic nutrients that pass out to sea through the inlet. A plan was put forward to develop a system to quantify the flow through the channel while simultaneously taking water samples in the PESC which would then be analyzed for these substances (the collection and analysis of these aforementioned water samples were carried out by another group and are not part of this report). NOAA's Atlantic Oceanographic and Meteorological laboratory (NOAA/AOML) developed the flow measurement system, which was deployed on March 16, 2009. The system continuously collected data at 6-minute intervals through June 5, 2011. An analysis of the water samples collected inside the PESC and in the coastal area adjacent to the PESC was used to describe the dispersion of water exiting the PESC into the coastal ocean on the ebb tide.

Port Everglades Shipping Channel (Ft. Lauderdale, Florida)

Figure 1. Location of the Port Everglades Shipping Channel.

2. Background

Previous studies undertaken by NOAA/AOML and others have shown that, on the ebb tide, water exiting from south Florida's coastal inlets can have a significantly higher level of nutrients and human source microbial contaminants than the water that enters on the flood tide (Carsey *et al.,* 2012). Data collected in the PESC prior to and during our study (e.g., Applied Coastal Research and Engineering, Inc., Kenneth Banks, Nancy Craig) indicate that the PESC can exhibit both vertical density stratification (Figure 2) and velocity stratification (an example of velocity stratification is shown as Figure 14). This implies that the potential exists for water masses, possibly of differing composition and occupying differing vertical positions in the channel, to be transported through the PESC at differing velocities, possibly even in opposite directions.

Techniques have been developed to estimate the flow through a channel using a fixed acoustic Doppler current profiler (ADCP) system (Ruhl and Simpson, 2005; Levesque and Oberg, 2012). These techniques require making a velocity measurement of a portion of the channel that can be related to a velocity that represents the mean velocity for the entire channel. This mean velocity, when multiplied by the channel area at the time of the measurement, gives the flux (Q):

$$Q = \text{channel mean velocity} \times \text{cross-sectional area at the measurement location} \quad (1)$$

The relationship between the fixed ADCP velocity measurement and the mean channel velocity is derived by collecting data across the entire width and depth of the channel with an independent down-looking ADCP system which is transected across the channel (this system will be referred to as the survey system in this report) and then constructing a mathematical relationship between the data from the two systems. Once this relationship is derived, velocities measured by the fixed system and estimates of the channel cross-sectional area can be used to generate an estimate of the flux rate (Q) through the channel. In considering the design for the PESC flow measurement system, it was necessary that this system be able to discriminate the flow velocities of vertically stratified water masses. This presented a significant design challenge and required a modified approach to collecting and applying calibration data from the survey system.

3. Flow Measurement System Design

3.1 Acoustic Design Considerations

Commercially-available ADCPs designed to make measurements inside a channel are typically deployed in one of two ways. In both configurations, a profile along the measurement axis of the instrument is generated by time gating the returning acoustical signal into "cells" or "bins." For a detailed introduction to ADCP principles, please refer to Teledyne RD Instruments (2006).

A vertical-looking system deployed to measure flow is typically placed on the bottom of a channel somewhere near the channel's center with the acoustic transmission paths arranged around the vertical axis. The advantages of this type of system are that the ADCP measures a vertical profile of velocities in the channel at the location where the instrument is deployed. In many cases, the velocities measured near the channel center are relatable to the mean channel velocity. These measurements can then be used to estimate the total volume transport through the channel (Ruhl and Simpson, 2005; Levesque and Oberg, 2012).

At Port Everglades, where the commercial and recreational traffic is heavy, the logistics of deploying equipment in the middle of the channel are very difficult. Furthermore, the effects of large, deep draft ships navigating the channel on a bottom-mounted system are unknown. The system needed for this study was expected to operate for at least one year, requiring connections to shore to power the system and retrieve data. Placing cables from the shore to an instrument located near the channel center would have been difficult and would have also increased the vulnerability of the system.

A second type of system used to measure velocities in a channel is the horizontal or side-looking ADCP. These systems are typically mounted somewhere near or on the side of the channel, at the mid-water depth, with the acoustic transmission paths arranged in a horizontal plane. These instruments generate a profile of velocities that represent the velocities that lie in this plane. The advantages of this type of system are that by mounting the system on or near the side of a channel, power and data cables can be kept short, and the difficulties of performing deployment
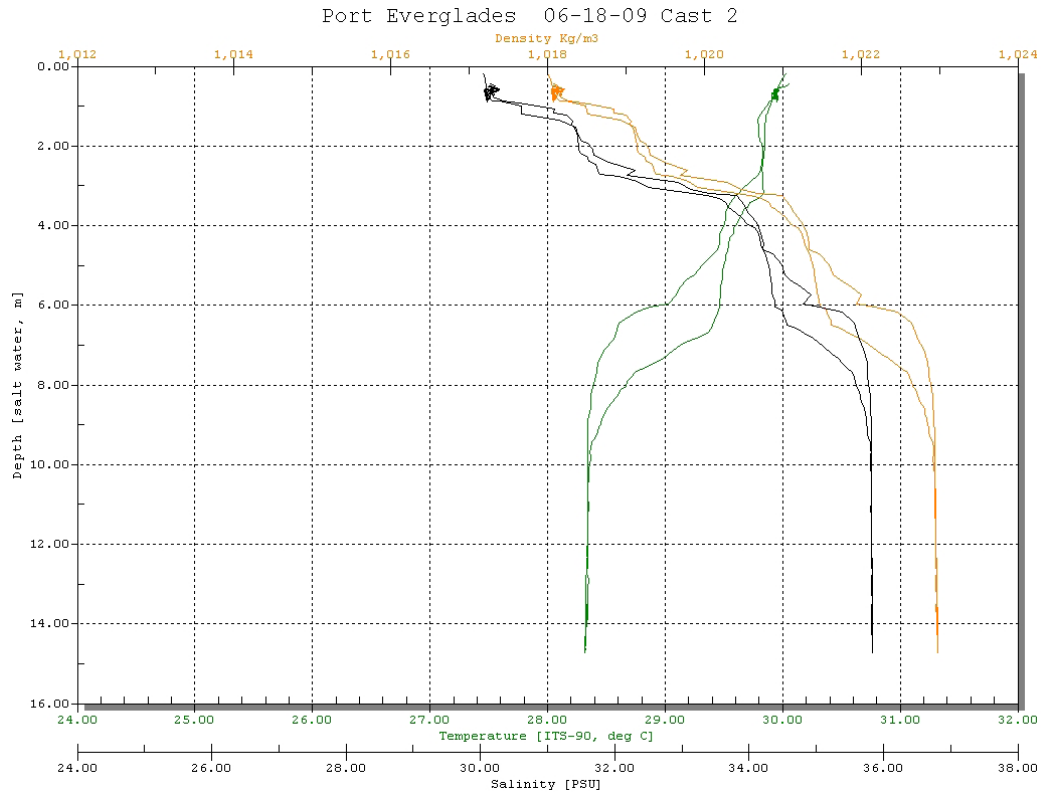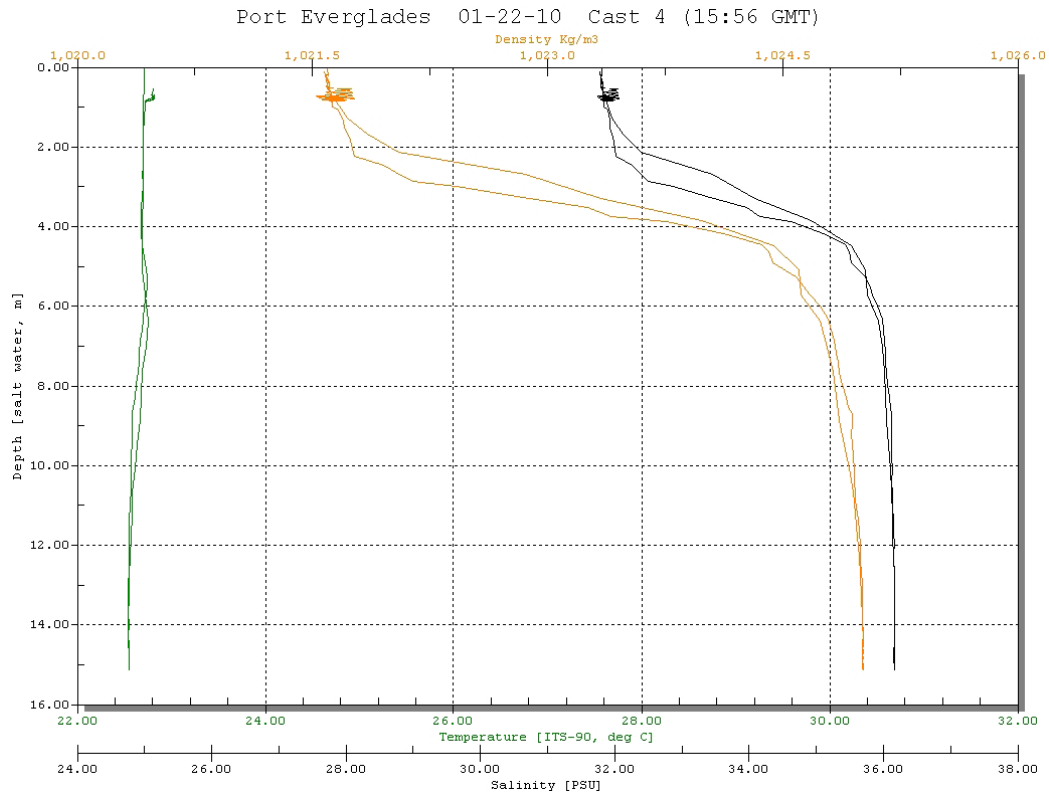
Figure 2. Two CTD casts from the Port Everglades Inlet showing less dense water near the surface.

and service operations inside an active shipping channel are minimized. A disadvantage of this type of system is that velocity measurements lie completely in a horizontal plane, and no information regarding the vertical structure of the velocities is available.

3.2 Hybrid System Deployment Configuration

The system developed for this study was a hybrid design that used a commercial, horizontal-looking ADCP (H-ADCP). Instead of mounting this instrument so that its beam plane lay in the horizontal plane, the instrument was deployed near the surface of the channel with the beam plane pointed down at a small angle so that each successive measurement cell would have a depth greater than the cell that preceded it (Figure 3). The optimal configuration would allow the beam plane to reach its maximum usable measurement depth somewhere near or beyond the channel's center. The Port Everglades Channel is approximately 241 m wide and 15 m deep at the measurement location. To achieve the optimal configuration, the system was mounted near one of the channel sides and pointed down at a small angle (5-10°). In planning this system, it was realized that acoustic signals propagating through a stratified environment would be refracted as the signals traversed regions of differing sound speed.

3.3 Acoustical Modeling

An acoustical modeling effort was undertaken to quantify the effects of refraction due to a vertically-stratified water column and to develop design criteria that would minimize the associated errors (Stamates, 2011). An acoustical ray trace model was constructed that used sound speed profiles generated from conductivity-temperature-depth (CTD) data taken in the PESC to predict the path of an acoustical "ray" launched at a specific angle by the iterative applications of Snell's Law (Eq. 2) where c_1 and c_2 are the sound speeds at the old and new positions, and θ_1 and θ_2 are the propagation angles of the ray at the old and new positions (Clay and Medwin, 1977).

$$\sin{(\theta_1)}/c_1 = \sin{(\theta_2)}/c_2 \qquad (2)$$

A ray launched at a given angle was propagated by some small distance, ΔX, and the new position of the ray segment terminus was then calculated. A new sound speed was
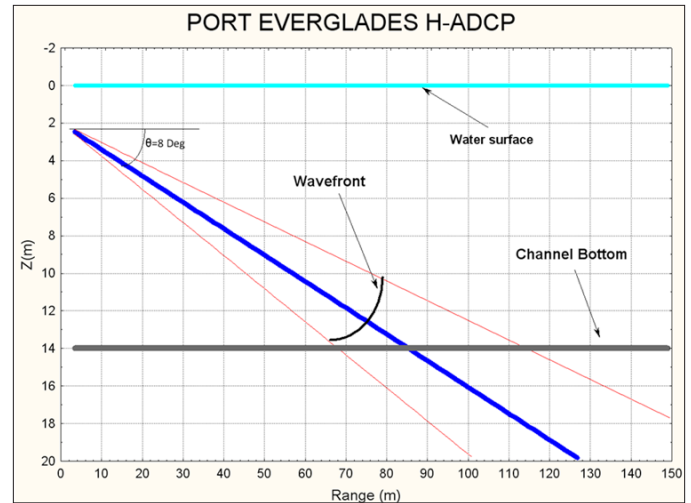
Figure 3. Schematic of the H-ADCP deployment configuration. The main acoustical beam is shown in blue, and the beam side lobes are shown in red.

calculated for the new position in the water column by interpolating the sound speed profile data and then, by the application of Eq. 2, the new propagation angle of the ray was calculated. This process was continued until the ray either reached a depth of 15 m or the ray was refracted such that it turned upward.

Input data for the modeling effort were provided by the Broward County Environmental Resources Division (Nancy Craig and Kenneth Banks, personal communications and unpublished data) and NOAA/AOML. The data used were chosen to represent a range of seasonal conditions.

Figure 4 shows the results of the ray trace model for two sound speed profiles chosen to represent the extremes of the conditions captured by the available data. Evaluating the modeling results for all of the available environmental data facilitated the selection of a launch angle, which was a compromise between the desire for the acoustic path to reach as far out into the channel as possible, balanced with the need for that acoustic path not to be significantly refracted when traversing the channel.

Figure 5 summarizes the results of the modeling effort. Along the x axis are the dates of the CTD casts that were used to generate the sound speed profiles. For each of these profiles, the range at which a ray hit the bottom at 15 m is given for the integer ray launch angles between 80-87°. From Figure 5 it can be observed that for shallow launch angles there is a large dispersion of distances for which a ray hits the bottom.
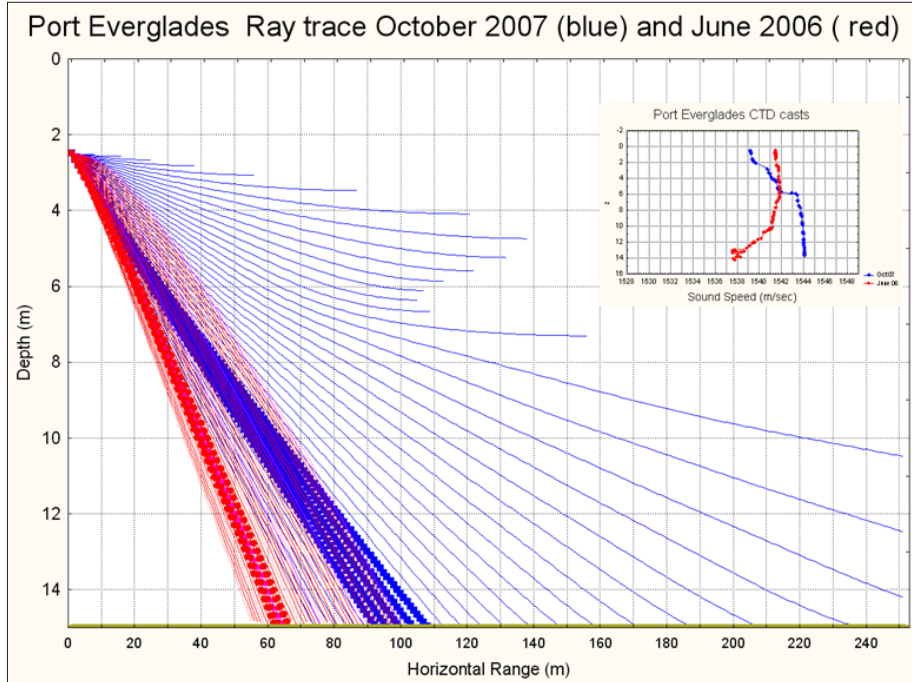
Figure 4. Ray trace diagram generated from two sound speed profiles which were chosen to represent the extremes of the conditions captured in the available data. The rays are the predicted paths of an acoustical signal projected from a source which has an infinitesimally small beam pattern at a specific angle. The angles represented by the rays are 80-89° with respect to the vertical.
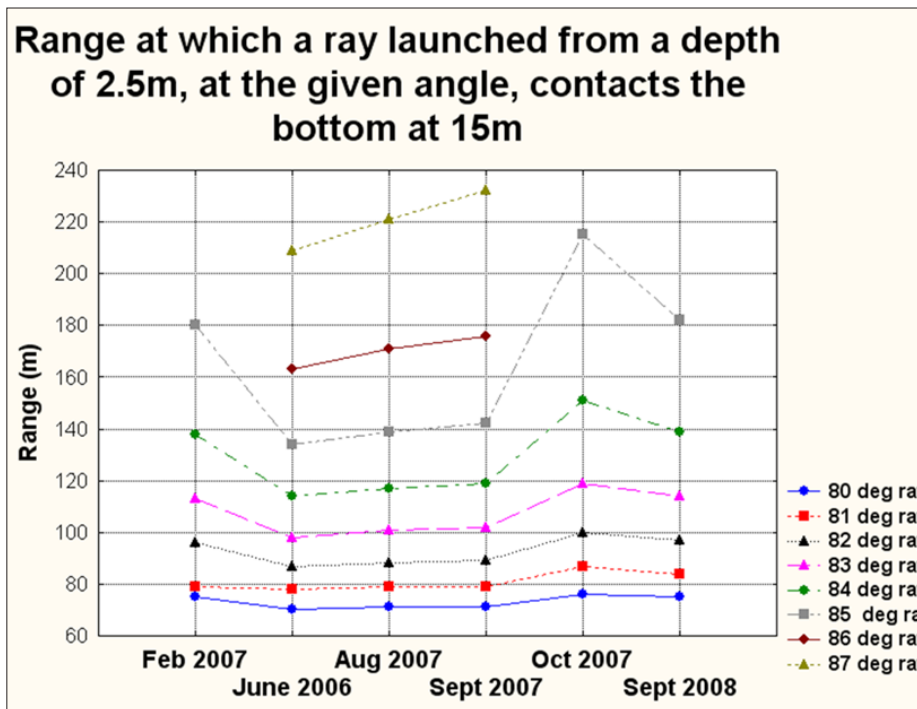
Figure 5. Summary of acoustical modeling results. The horizontal distance at which a ray strikes the bottom at 15-m depth is given at launch angles between 80-87° for each of the available sound speed profiles.

The rays launched at 86-87° did not reach the bottom for the February 2007, October 2007, and September 2008 sound speed data. These rays were refracted upward. As the launch angle became less shallow with respect to the horizontal, the distance at which a ray hit the bottom became more similar for all of the environmental sound speed data. After evaluating the results of the modeling effort, an angle of 8° down from the horizontal was chosen as the design target.

3.4 Instrument Selection

The modeling results presented in section 3.3 idealize an acoustic signal as a ray of infinitely small width. In fact, an acoustic signal transmitted from a transducer has width, and the transmitted acoustical pulse diverges (becomes wider) as it travels away from its source. Because of this divergence, the backscattered energy returning from measurement cells farther from the instrument is generated by a larger volume of water than that from cells closer to the instrument. Furthermore, while the majority of the energy transmitted from the transducers is focused into the main beam, some fraction of the energy is transmitted into alternate paths called side lobes. These side lobes have a significantly wider beam angle than the main beam and, while there is less energy contained in the side lobes, signals returned from the side lobes affect the velocity estimates. If the returned signal from the side lobes has contact with the surface, bottom, or any other fixed boundary, the velocity measurement can be biased. Therefore, the position of the side lobes in the measurement space had to be considered when configuring the system (Figure 3). To minimize these effects, an instrument equipped with transducers that minimized beam divergence and the width of the side lobes was desirable.

Of the commercially available ADCPs suitable for this application, the Teledyne RD Instruments 300-kHz H-ADCP with 25-cm transducers was chosen. These transducers are specified to have a main beam width (defined as the angle at which the energy level is one half that which is present along the axis of the transducer) of ± 0.43° and side lobes whose width (defined in the same manner as the main beam) is 1.88°. This instrument uses three acoustic transducers aligned in a plane. The central transducer defines the central measurement axis of the instrument, while the other two transducers are angled 20° to the right and left of the central transducer. This system reports velocity data in two dimensions which lie in the plane of the beams. An algorithm contained in the instrument corrects the data for the tilt of the beam plane so that the resultant velocities reported by the instrument are equivalent to those lying in the horizontal plane at the position of the measurement cell.

3.5 Site Selection

The system deployment location was chosen based on design constraints and the availability of existing resources. Ideally, the flow measurement system needed to be mounted at a location where the channel geometry was relatively uniform with parallel boundaries. However, there were only limited sections of the PESC where this was the case. The bathymetry of the PESC dictated that the system be placed somewhere near the main channel so that the acoustic beams and side lobes did not contact the bottom before reaching the maximum desired measurement depth (Figure 6). The Instrument needed to be located below the water's surface at a sufficient depth so that interference from the surface did not impact the performance of the system (which precluded
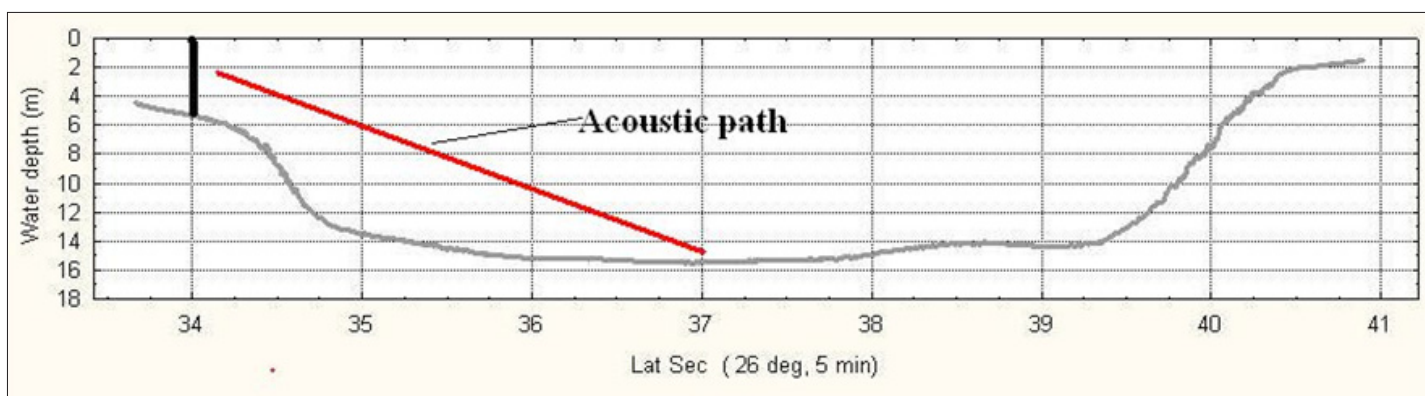

Figure 6. Port Everglades Shipping Channel bathymetry with schematic of the acoustic path.

mounting the instrument on the seawalls on either side of the channel) but yet still allowed the majority of the water column to be measured.

A team of divers from AOML inspected areas identified as possible locations for the placement of the acoustical system. The dive team reported that the bottom and sides of the bank of the main channel were unstable and not suitable for installing a mounting structure at these locations. On the south bank of the PESC, the United States Coast Guard (USCG) maintains a navigation marker located at the edge of the main channel (USCG #7, 26.0928°N, 80.1089°W). This navigation marker is just offshore of the United States Naval Surface Warfare Center Ocean Measurement facility. Permission was granted by the USCG to mount the instrument on the navigation marker. Permission was also granted from the U.S. Navy to place the shoreside components of the system at the Ocean Measurement facility.

3.6 Survey System

To make measurements of the channel bathymetry and of the water velocity structure throughout the channel, a 1200-kHz Teledyne RD Instruments Rio Grande ADCP, along with the Teledyne RD Instruments survey software, WinRiver II, were used. The instrument was deployed via a fixed mounting (U.S. Geological Survey, 2001) from the side of a small boat (Figure 7). After deploying the instrument from the side of the vessel, the depth of the transducers below the water surface was measured and entered into the survey software.

The instrument contains an internal compass which gives the orientation of the system relative to magnetic north. The compass was calibrated before each survey effort using procedures specified by the manufacturer. The magnetic declination for the area (6°W) was entered into the survey software so that the processed velocity data were relative to true north. A differential global positioning system (GPS) was connected to the survey software for the location where each measurement was made to be recorded along with the measurement.

The ADCP transmitted a coded acoustical signal from the four beams, each of which was angled 20° from vertical.

Figure 7. Vessel equipped with down-looking, 1200-kHz ADCP used to survey the Port Everglades Channel bathymetry and collect calibration velocity data.

The instrument then received the backscattered signal from particles in the water or the reflection off the bottom. To calculate bathymetry, the system calculated the distance along each of the beams from the instrument to the bottom. The survey software corrected these data for the beam angle and system tilt and roll and then calculated the depth vertically below the system. To calculate water velocity, the radial Doppler velocities along each beam, returned from particles suspended in the water column (assumed to be moving at the same rate as the water), were calculated. The data were corrected for system tilt and roll, and a three-dimensional water velocity estimate was calculated.

The system derived the velocity of the survey vessel by estimating the apparent velocity of the bottom relative to the vessel (this is actually the vessel's motion relative to the bottom). This "bottom track" velocity was then used to correct the water velocity measurement for the vessel's motion. Like the fixed system H-ADCP, the survey system ADCP was capable of making velocity measurements in bins located throughout the water column. As configured for this application, the system made three-dimensional velocity measurements in 0.25 m bins starting 1 m from the surface and extending down to within 1 m of the bottom. As configured and mounted on the small boat, this system was capable of making measurements of nearly the entire vertical and horizontal extent of the PESC.

3.7 System Installation

A mounting structure was designed and built to attach the acoustical system to the USCG navigation marker. This mounting structure allowed for horizontal and vertical adjustment of the beam plane once the instrument was attached to navigation marker. On March 16, 2009, the system was deployed by AOML personnel on the shoreside and by commercial divers performing the underwater work (Industrials Divers, Inc., Ft. Lauderdale, Florida).

The instrument was deployed at a depth of 2 m relative to the mean water level (Figure 8). The mounting was adjusted by the divers to be level and pointed due north across the channel (the Port Everglades Channel is oriented almost exactly east-west at the measurement location). The instrument was then adjusted for the beam plane to tilt down at an angle of 8°. At the same depth as the H-ADCP, a conductivity and temperature sensor was deployed.

Power and data cables were laid across the channel bottom, protected with sand bags, that terminated on shore at the U.S. Navy Ocean Measurement facility. At the location of the terminus of the data and power cables, a waterproof enclosure was mounted to an existing structure. This enclosure contained the cable terminations, shoreside data loggers, and power conditioning equipment. Adjacent to this structure, a Vaisala WTX 520 instrument with a suite of meteorological sensors was also installed (Figure 9).

Data from the H-ADCP were recorded to the onboard data logger and recovered by connecting a computer to the cable
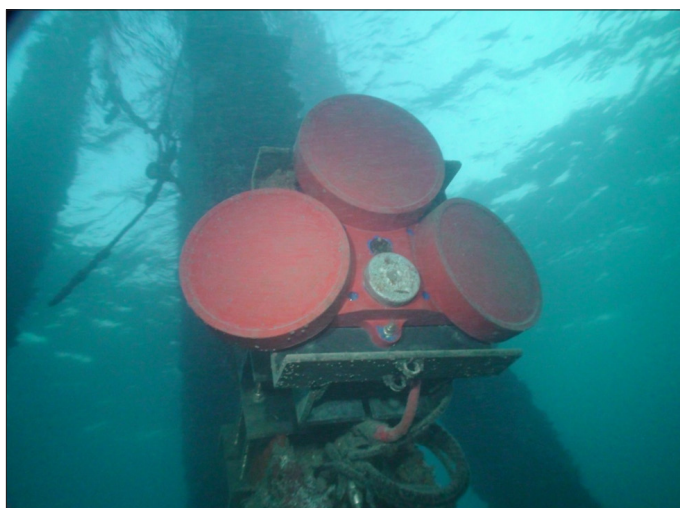
Figure 8. H-ADCP mounted on the USCG navigation marker.
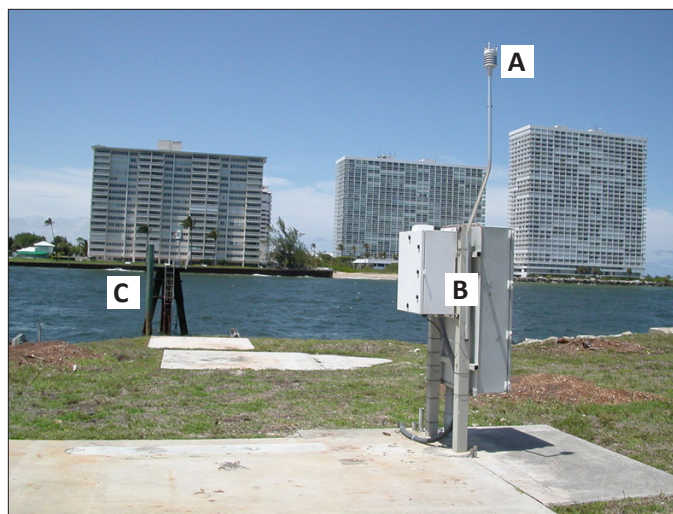
Figure 9. Installation of flow system: (A) meteorological sensors; (B) power and data loggers; and (C) navigation marker to which the H-ADCP was attached.

terminus at monthly intervals. Data from the other sensors were logged to a Campbell Scientific data logger model CR1000. Data were recorded from all sensors at 6-minute intervals. A battery power backup system was incorporated into the power supply design to enable the system and all the sensors to remain operational for at least 72 hours in the event of a power failure.

Data from the meteorological sensors were also transmitted via satellite to AOML where they were then reported to NOAA's National Data Buoy Center (NDBC). These data were made publicly available via the NDBC web site as station PVGF1 (http://www.ndbc.noaa.gov/station_page.php?station=PVGF1). Although the flow measurement sensor was disabled by a cable failure in June 2011 and removed, the meteorological sensors remained in place and were still actively reporting data as of April 2013.

3.8 H-ADCP Configuration

The H-ADCP was programmed to provide a measurement of the currents at 6-minute intervals. Each measurement was an ensemble average of 460 acoustical transmissions spread across the measurement interval. The instrument was set to collect data in 1.5-m bins with the center of the first bin located 3.45 m from the transducers. In this configuration, with the plane of the beams set at a down angle of 8°, the location of the center of each bin was 1.48 m farther than the preceding bin in the horizontal plane and

0.208 m deeper than the preceding bin in the vertical plane (Figure 3). This small vertical change from bin to bin allowed for good resolution and a redundancy in measurements of the vertical structure. With these settings, the estimated standard deviation of a velocity measurement was predicted to be less than 0.5 cm/s.

4. Results

4.1 H-ADCP Data

Initial data returned from the H-ADCP system were examined to assess the system's performance. Inspection of these data provided evidence that the system was adequately resolving the structure in the vertical and gave an indication of where the data were being influenced by side lobe interference from the beams impacting the bottom. The effect of the side lobes impacting the bottom appeared to begin in bin 40. To assure that only data free from side lobe interference were used, bins 1-36 were used for analysis. A contour plot of velocity data from the system was generated with depth on the vertical axis and time on the horizontal axis (Figure 10). The measurement location of the center of bin 1 was 3.4 m from the instrument in the horizontal plane, and the depth of the measurement point of bin 1 relative to the mean water level was 2.5 m. The measurement location of the center of bin 36 was 55 m from the instrument in the horizontal plane, and the depth of the measurement point of bin 1 relative to the mean water level was 10.1 m.

An examination of data returned from the system provided information about how the ebb and flood tidal flows

Figure 11. Time series of data from the flow system showing the surface layer velocity, the deep layer velocity, and the depth of the H-ADCP pressure sensor.

developed inside the channel. A time series of the surface and bottom layers, along with the depth of the instrument, is shown in Figure 11. In this representation, the surface is the average of the velocities from bins 1-3. This represents a depth of 2.6-3.2 m relative to the mean water level. The bottom layer is represented by the average of bins 24-36, which represents the depths of 7.5-10.2 m relative to the mean water level. From Figures 10 and 11, a few observations can be made. During ebb tide, the surface layer was sometimes seen to lead the bottom layer into the ebb phase by a short period of time. Near the end of an ebb tide, the bottom layer would begin to flood while the surface layer was still in ebb; therefore, surface water was exiting the inlet towards the ocean while, at the same time, ocean water was entering the inlet in the deeper parts of the channel. The highest velocities in the surface layer were often observed near the beginning of the ebb tide. This complex behavior was variable and may be related to the lunar phase, winds, offshore waves, and the quantity of water entering the Port Everglades basin through its tributaries and from surface runoff.

4.2 Establishment of the Instrument's Position in the Water Column

To estimate the cross-sectional area of a tidally-influenced channel, a measurement of the water level relative to a reference water level is necessary. The H-ADCP system is

Figure 10. Contour plot of data from the H-ADCP system.

equipped with a highly accurate pressure sensor, the data from which are reported with each measurement. Before deployment, this sensor was zeroed and the atmospheric pressure at that time was recorded. Once the system was deployed, atmospheric pressure data from the meteorological sensors were used to compensate the pressure sensor for the varying atmospheric pressure. Once corrected in this manner, the pressure sensor provided a measurement of the height of the water column above the instrument.

During deployment of the system, tide tables were used to guide the dive team in positioning the instrument at the desired depth below the mean water level (2 m). To confirm this depth and improve upon its accuracy, a physical survey of the instrument relative to nearby benchmarks was attempted. This proved difficult to accomplish to the desired accuracy so a second technique was used. A tide program, Nobeltec Tides & Currents, capable of calculating the tidal height relative to a nearby tide station was used to generate a 216-day time series of tidal heights at a tide station inside the Port Everglades basin at the same intervals as the instrument was making measurements of the water level (6 minutes). The mean of the difference between these data and the readings from the instrument's corrected pressure sensor was calculated, and this became a secondary correction to the pressure data. These corrections allowed for the accurate positioning of the instrument with respect to the mean sea level. The instrument's position relative to mean sea level was calculated to be 2.095 m.

4.3 Channel Cross-Sectional Area Function

To accurately estimate the flux of water across a given cross section of a channel, an accurate estimate of the channel cross-sectional area at the measurement location must be known. For this application where the water column was subdivided into layers, the cross-sectional area of each of the layers must be known. To accomplish this, the survey system was slowly transected across the channel perpendicular to the channel axis at the location of the H-ADCP installation. Four transects deemed to be of the best quality were extracted, along with the positional data from the GPS. These four transects were averaged together and smoothed. This was done to average the differences in the bathymetry data that resulted from the survey vessel traveling along slightly different paths across the channel.

Figure 12 shows the four transects and the resultant smoothed bathymetric contour. The averaged bathymetry and position data were then interpolated as a function of depth with the width of the channel being calculated for the depths that corresponded to each bin of the H-ADCP system. The width of the channel at 11 depths lying above the first bin of the H-ADCP system was calculated as well. After calculating the width of the channel at each of these depths, these values were multiplied by the height of a fixed system bin (0.208 m), giving a cross-sectional area of the channel corresponding to the depth of each of the fixed system bin depths (and depths above the instruments). From these calculations, it was estimated that the channel cross-sectional area at the mean water level was 2651 m^2. At the location of the H-ADCP installation, the channel is bounded by seawalls on both the north and south sides. The correction to the cross-sectional area that was applied for changing water levels was equal to the difference from the mean water level as measured by the corrected pressure sensor of the H-ADCP multiplied by the channel width (240.9 m).

4.4 Calibration

The H-ADCP system makes measurements of the water velocity in discreet bins along the plane defined by the path of the three acoustical beams. As previously described, the beam plane begins at the instrument which is near the surface and continues away from the instrument, pointed down at an 8° angle (Figure 3). Each measurement bin returns data that correspond only to a specific location along the beam plane. To relate these measurements to a mean channel velocity for the entire channel or for vertical subsections of
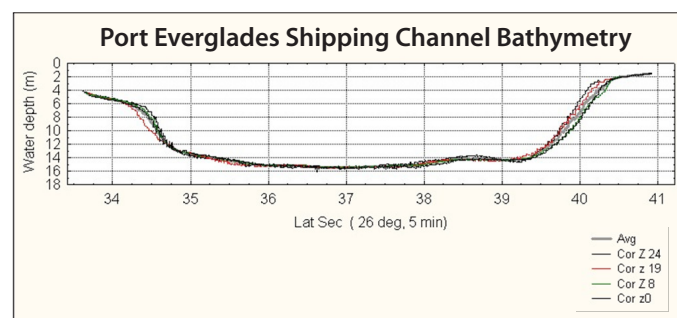

Figure 12. Port Everglades Channel bathymetry. The bathymetry profile is an average of four transects across the channel. The distance across the channel is expressed as latitude seconds.

the channel, a series of calibration exercises was carried out using the survey system described in section 3.6. During these calibration exercises, the survey system was repeatedly transected across the PESC throughout a flood or ebb tide. These transects provided velocity data for nearly the entire channel.

Figure 13 is an example of the velocity data from the survey system and clearly shows the vertical structure in the velocities. Two wooden pilings located on the north and south sides of the channel were used as references for transects to be conducted in a repeatable manner. The distance from these pilings to the nearest seawall was measured with a laser range finder and entered, along with the estimated bottom geometry from the pilings to the channel boundary, into the WinRiver II software (the south bottom geometry from the marker to the south seawall was modeled as rectangular, whereas the north side bottom geometry was modeled as triangular).

Four of these calibration exercises were carried out on the ebb tide and two were carried out on the flood tide (Table 1). In total, 289 calibration transects were made. An emphasis was placed on the ebb tide, as this is the tidal phase that has the potential to advect anthropogenic materials into the coastal ocean. Two of the ebb tide calibrations and one of the flood tide calibrations were carried out near the spring tide. The other calibrations were conducted near the neap tide.

This technique of using a transected down-looking survey system to calibrate a fixed, cross-channel ADCP system is described in Huang (2006) and Levesque and Oberg (2012) and is referred to as the "index velocity method." A significant difference between the index velocity method and what was necessary to perform the calibration of this
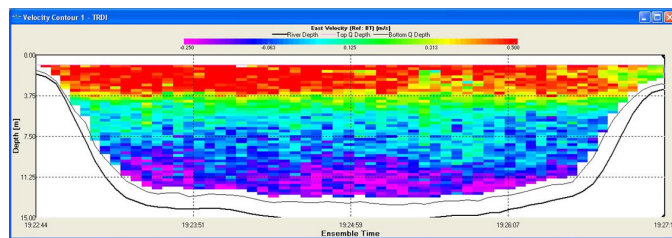

Figure 13. Example of velocity data from the survey system showing the vertical velocity structure.

system, however, is that the index velocity method typically integrates velocity measurements from the transected system in the vertical and horizontal to derive a single, channel-averaged mean velocity. The relationship between this integrated velocity and a velocity measured by the fixed system is then calculated so that the velocity measurements by the fixed system can be used to estimate the channel-averaged velocity. In this application, however, it was desired to estimate the channel-averaged velocity for vertical subsections of the channel.

After assigning a depth relative to the mean water level to each bin of velocity data from the survey system, the velocity data were then horizontally averaged to estimate the average channel velocity at that depth. Vertical averages were then constructed from these data. Velocity measurements from the fixed system were smoothed using a three-point running mean filter and then interpolated in time so that the time of the fixed system data corresponded to the median time of the channel crossing by the survey system. Vertical averages from the fixed system were constructed that corresponded to the vertical averages made from the survey system data. In other words, an estimate of the mean velocity for a particular vertical section of the channel, at a particular time, was constructed from data from both systems. Using methods

Table 1. Port Everglades H-ADCP calibration exercises.

Calibration Number	Date	Time Start (UT)	Time End (UT)	Tidal Phase	Lunar Phase
1	June 18, 2009	11:35	15:08	Ebb	Four days until new moon
2	July 7, 2009	13:34	19:29	Ebb	Full moon
3	September 23, 2010	16:47	21:53	Ebb	Three days until first quarter
4	November 16, 2009	13:49	19:03	Ebb	New moon
5	January 22, 2010	12:50	18:45	Flood	First quarter
6	May 25, 2010	18:45	00:04 (May 26)	Flood	Two days past full moon

described in section 4.5, relationships were built using these two data sets which then allowed the mean velocity for the vertical subsections of the channel to be estimated from the velocities measured by the fixed system. The mean velocity estimates for these vertical sections or "layers" were then multiplied by the area of those layers, and a flux, or Q (Eq. 1), for those layers was estimated.

4.5 Vertical Subdivision of the Channel

Decisions regarding the vertical subdivision of the channel were made based on density and salinity data from the CTD casts, velocity data from the fixed system, data collected with the survey system, and a co-analysis of the data from the fixed and survey systems. These data sets showed that there was significant variability in the velocity and density structures of the channel and that the flood and ebb tidal phases of the channel showed significant differences in their vertical structure. This is not unexpected. During the flood phase, seawater from offshore is drawn into the channel. On the ebb phase, some mixture of the seawater from previous flood phases and fresher, possibly nutrient-laden water, is advected out of the PESC towards the ocean. The fresher inland waters would presumably be less dense and located at the top of the water column.

Rainfall, surface runoff, and water released by control structures modulate the quantity and density of this inland water. The CTD density data suggested a two-layer system with the depth of the break between the upper and lower layers being between 3-6 m (Figure 2). Using a six-month record of velocity data from the fixed system, the mean, standard deviation, and minimum and maximum velocities were plotted as a box and whisker diagram for the flood and ebb tides (Figure 14). The profile of velocity means for the ebb tide shows a velocity maximum near the 4-m depth. The standard deviation increases with depth. During the flood tide, the mean velocities are largest at roughly the 8-m depth. The standard deviation also increases with depth, but this is not as pronounced as during the ebb tide. The mean velocity assigned to the uppermost bins during the flood tide was near zero. This was attributable to the surface layer beginning to flood (traveling in a westerly direction) at a later time than the lower layer and, in some cases, the upper layer remaining in ebb condition (traveling easterly) for the majority of the flood tide interval.
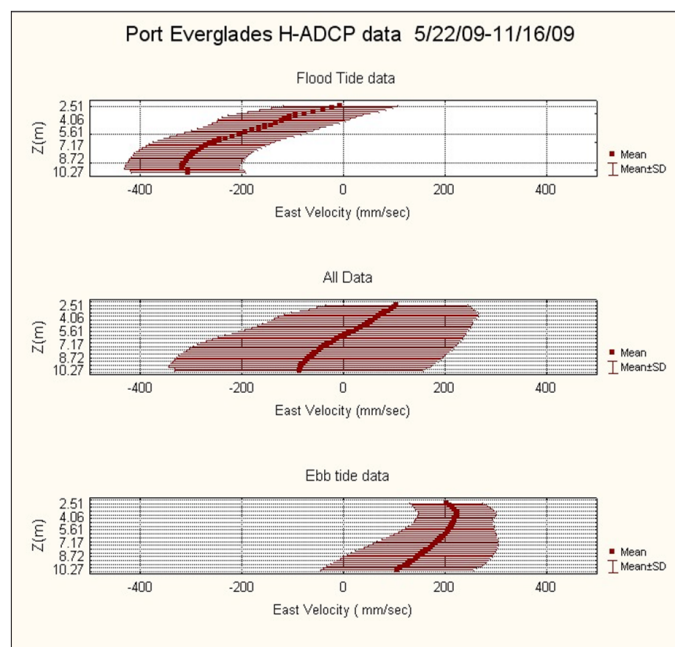

Figure 14. Box and whisker plots showing the mean and standard deviation for data collected from the H-ADCP over the period of May 22, 2009 through November 16, 2009. Data are shown for the ebb tide, flood tide, and all data.

It was considered prudent to keep the division of the channel as general as possible yet still provide the pertinent information. Modeling the channel as a two-layer system was supported by the CTD cast information. Choosing the fixed system bins to represent these layers (the index velocity method specifies that the fixed system measure a representative velocity, not the entire velocity structure) was guided by analysis of the velocity structure. When performing the analysis of the calibration data, many other vertical subdivisions and combinations of these subdivisions were attempted and evaluated; however, it was found that little or no improvement was made by expanding beyond a two-layer system. The surface layer was defined as the water lying above the depth of the fixed system bin 4. This depth is very near 3 m relative to the mean water.

4.6 Calculation of Index Relationships

It should be mentioned that the vertical sectioning of the PESC described in section 4.5, the derivation of the equations discussed in this section, and the calculation of Q discussed in section 4.7 were not performed independently. Many different combinations of vertical layers for the

fixed and survey systems were constructed and tested to determine if the data from the fixed system could reproduce the velocities reported by the survey system. These velocity equations were then tested to determine if a Q calculation could be made that was in good agreement with the Q estimates from the survey system.

A data set from the six calibration exercises was constructed containing the horizontally-averaged velocities from each available depth from the survey system. Each bin of the fixed system velocity data was smoothed using a three-point mean filter and resampled in time via linear interpolation so that its time matched the median time of the corresponding survey system transect. Parameters derived from the survey system data such as the transect averaged mean channel velocity, the channel area estimate, and the total Q for each transect were included in the data set, as were data from the conductivity and meteorological sensors.

Inspection of these data showed periods of close agreement with the channel velocity estimates from the two systems and also periods where the systems showed significant differences. It was observed with the survey system that the channel velocity structure could become incoherent along a particular horizontal layer (Figure 15). The fixed system measures only at one point for a particular depth and would not have the ability to sense and then compensate for these occasions of horizontal incoherence. Recognizing that data from these periods when the systems were clearly in disagreement would bias the results if included in the regression calculations, certain data from the calibrations were excluded from the analysis.

For the deep layer, a regression was calculated using the fixed system velocities at a depth of 7.9-9.9 m. A regression relationship was calculated using data from calibration exercises 2-6 (flood and ebb tides). This resulted in a regression with a linear correlation coefficient of
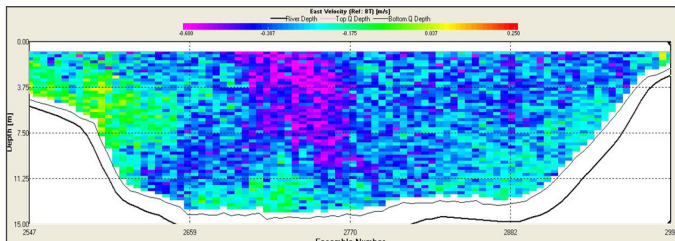
$R^2 = 0.9680$ (Figure 16). Differences in the velocity profiles observed near the surface during flood and ebb tides (Figure 14) suggested that constructing separate regressions for the flood and ebb tides would provide more robust estimates of the surface layer. For the surface layer during the flood tide, data in the depth range of 2.5-2.9 m from the survey and fixed systems were used to derive the regressions. This resulted in a regression with a correlation coefficient of $R^2 = 0.9214$ (Figure 17). For the ebb tide, data from the survey system in the depth range of 2.5-2.9 m was regressed with data from the fixed system at a depth range of 4-4.5 m.
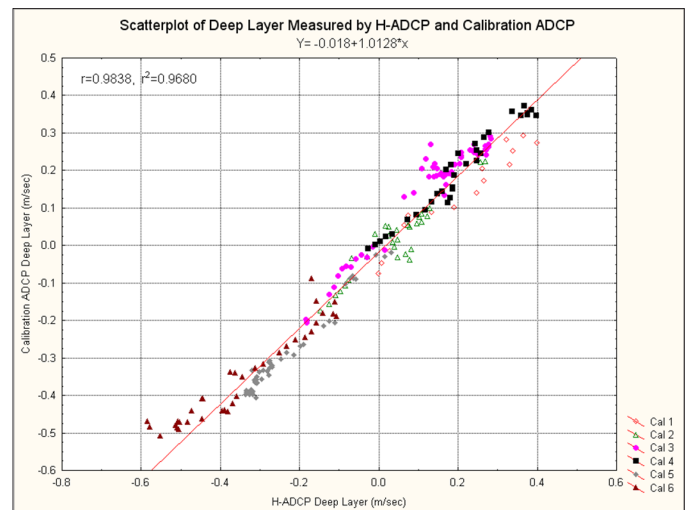

Figure 16. Deep layer regression plot of data from the survey and H-ADCP systems.
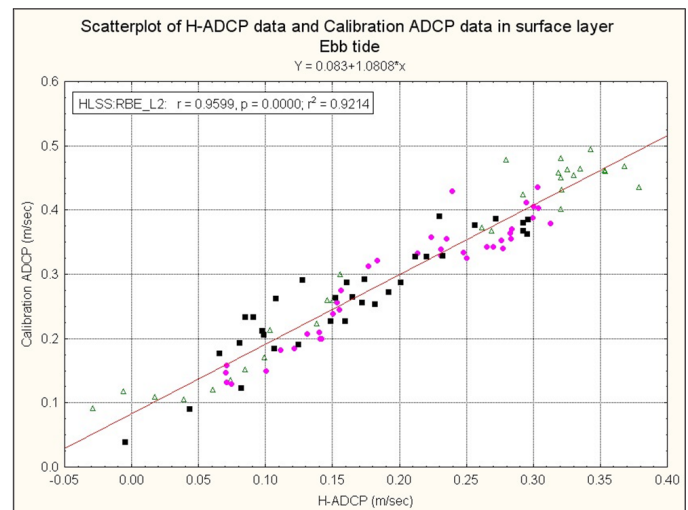

Figure 17. Shallow layer regression plot of ebb tide data from the survey and H-ADCP systems.

Figure 15. Velocity data from the survey system showing inhomogeneities in the flow.

This resulted in a regression with a correlation coefficient of $R^2 = 0.793$ (Figure 18). The use of data from different depths for the survey and fixed systems was done for the flood tide, as it appeared that the fixed system was not capturing a reliable velocity measurement in the upper bins (again, the index velocity method requires only that the velocity measurement from the fixed system is relatable to the desired mean velocity).

Figure 19 shows the surface and deep velocities measured by the survey system and the velocities calculated from the fixed system data. The residuals between the calculated mean velocities from the fixed system and the velocities from the survey system were calculated, and the distribution of these residuals is plotted in Figure 20. Figure 21 shows a time series of these residuals, along with a plot of the north component of the wind speed. Figure 21 suggests that the forcing of the wind may explain some of the observed discrepancies. In an effort to improve upon these results, regression models were constructed that incorporated forcing of the wind on the channel. The north and east wind vectors and their squared values were used in various multiple regression calculations. The distribution of the residuals from the models, including and not including the wind, is shown in Figure 22. From this it was observed that the incorporation of wind into the regression equations improved model accuracy only slightly.
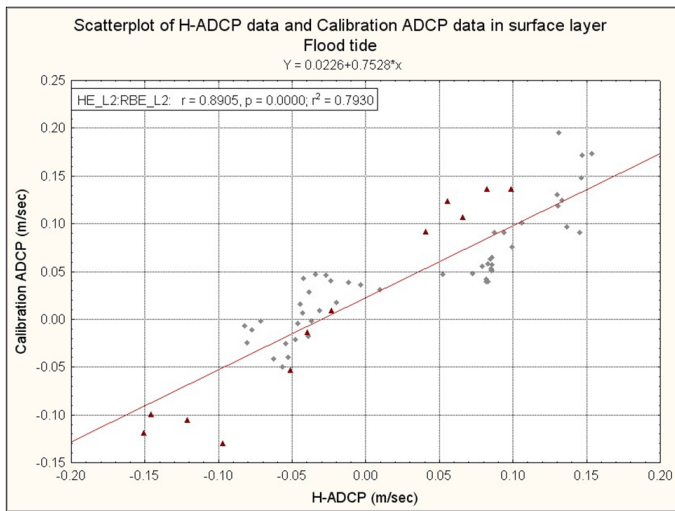

Figure 18. Shallow layer regression plot of flood tide data from the survey and H-ADCP systems.
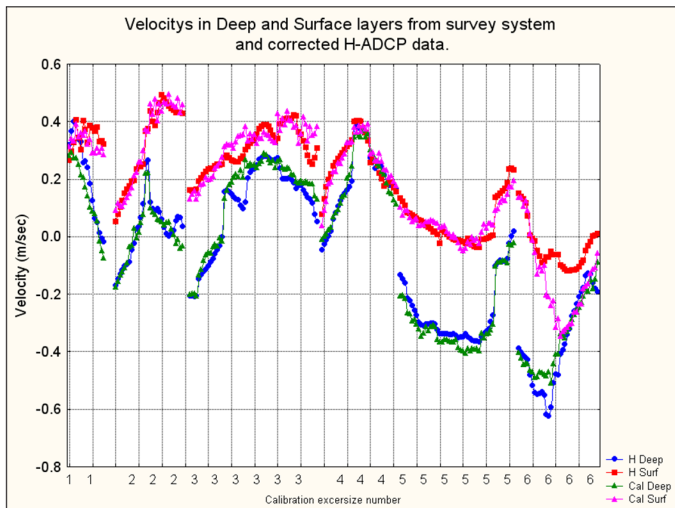

Figure 19. Velocity data from the survey system and corrected velocity data from the H-ADCP system.
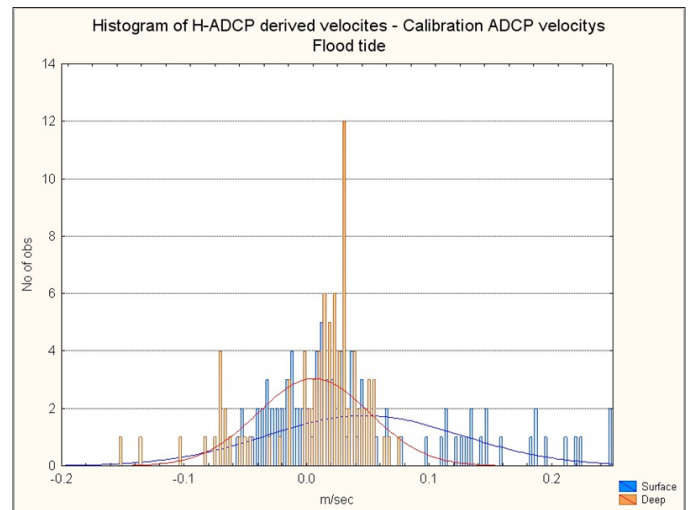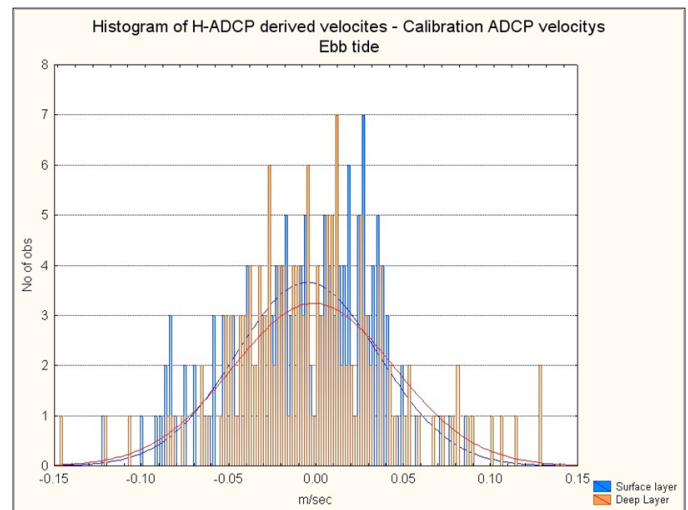

Figure 20. Histograms depicting the distribution of the differences between velocities predicted by the H-ADCP system and those measured by the survey system for the flood and ebb tides.
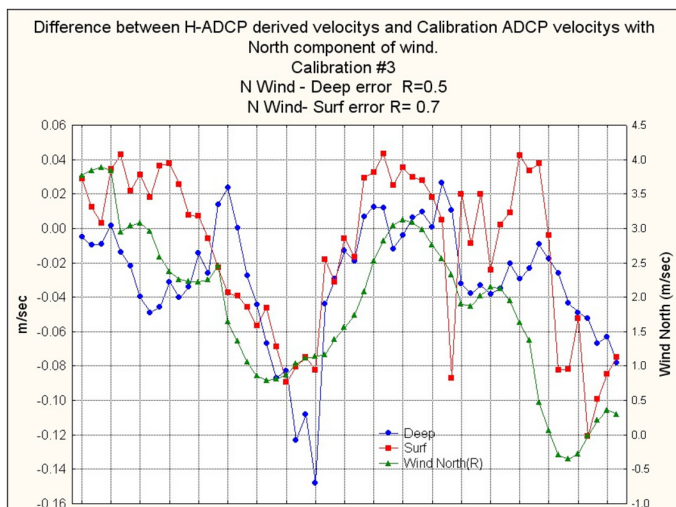
Figure 21. Time series of the difference between H-ADCP derived velocity data and velocity data measured with the survey system. The value of the north component of the wind is also plotted. Correlations between the residuals and the wind are given for the deep and surface layers.
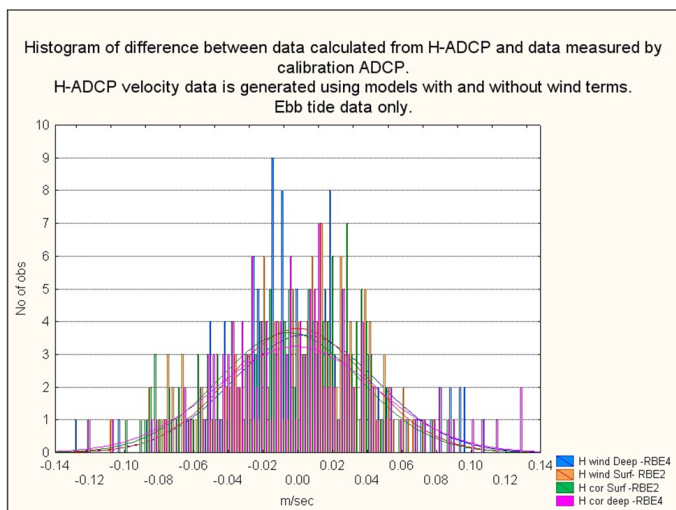

Figure 22. Histogram depicting the distribution of the difference between velocity data generated using the H-ADCP system with and without wind corrections and the velocity from the survey system.

4.7 Calculation of Q

To calculate the volume of water transported through the inlet per unit of time, the mean velocity estimates for the surface and bottom layers were multiplied by the area function for those layers. In the case of the bottom layer, the area function was a constant. In the case of the surface layer, it was everything above the layer demarcation. Once these calculations were made, the Q for the individual layers

and the total Q (the combination of the surface and bottom layers) were compared to the Q estimate made by the survey system. Figure 23 shows histograms of the surface and bottom layers of Q for data from May 22, 2009 through March 4, 2011. The surface layer distribution shows that more water flowed seaward in the surface layer than flowed landward. The deep layer distribution is more symmetric but has a net average landward flux. This is consistent with the velocity data shown in Figure 11.

4.8 Calculation of Total Volume Transport Per Tidal Phase

To estimate the total volume of water exiting the inlet on a particular tidal phase, a ten-point running filter was applied to the surface layer Q and deep layer Q data for June 1, 2009 through May 31, 2011. The measurement where the Q calculation changed sign was used to identify the beginning and end of a particular tidal phase (in that layer). The time that lapsed between the points identified as the start and end of a tidal phase was recorded, and the difference between these times was used to estimate the duration of the particular tidal phase. Histograms for the periods of the tidal phases are shown in Figure 24, and statistics are given in Table 2. Between the start and the end of a tidal phase, Q values were multiplied by the sample interval (360 sec) and summed over the tidal phase to give a total volume transport in that layer for that tidal phase. These transport data are shown as histograms in Figure 25, and statistics of these data are given in Table 2.

The tidal data showed that the periods of the ebb and flood were similar for the deep layer but markedly different for the shallow layer. The surface layer was in flood phase much less than in ebb phase. The statistics of the volume per tidal phase data were calculated for each month and are presented in Figure 26 and Table 3. An increase in volume transport in the surface layer ebb flow was observed during the months June through September, which corresponds to the rainy season in south Florida.

4.9 Meteorological Forcing of the Inlet

Ft. Lauderdale International Airport is located 4 km from the Port Everglades Inlet. The monthly rainfall rates recorded at Ft. Lauderdale International Airport and distributed by
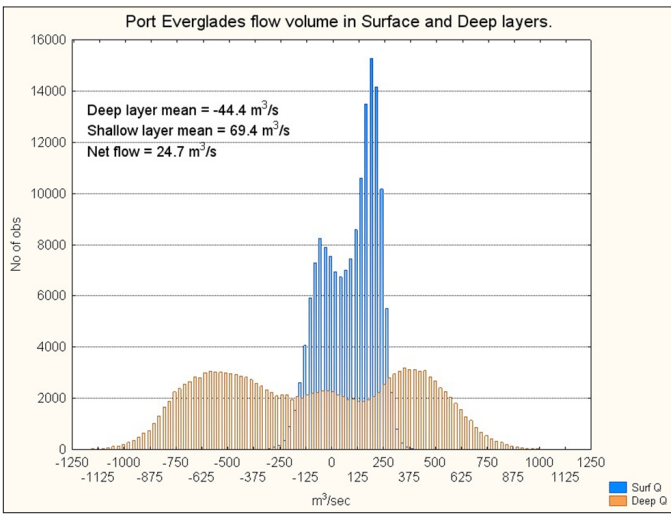
Figure 23. Histograms of Q calculated for the surface and deep layers. Positive values are seaward. Data are for May 22, 2009 through March 4, 2011.
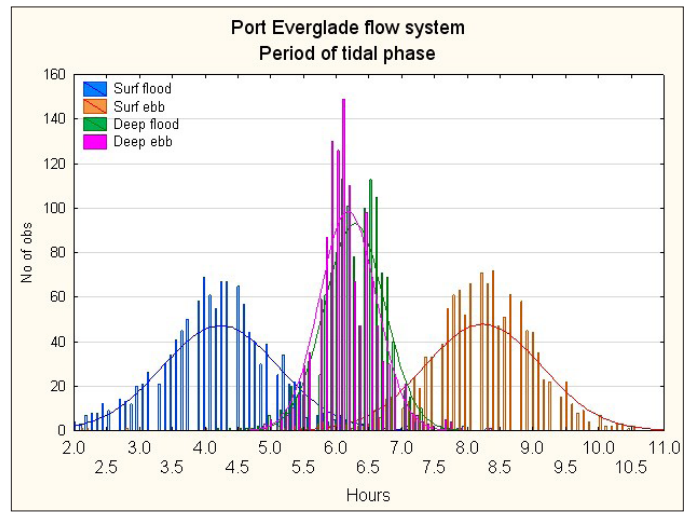
Figure 24. Histograms of the ebb and flood tidal phases for the surface and deep layers. These calculations were made from data from June 1, 2009 through May 31 2011.
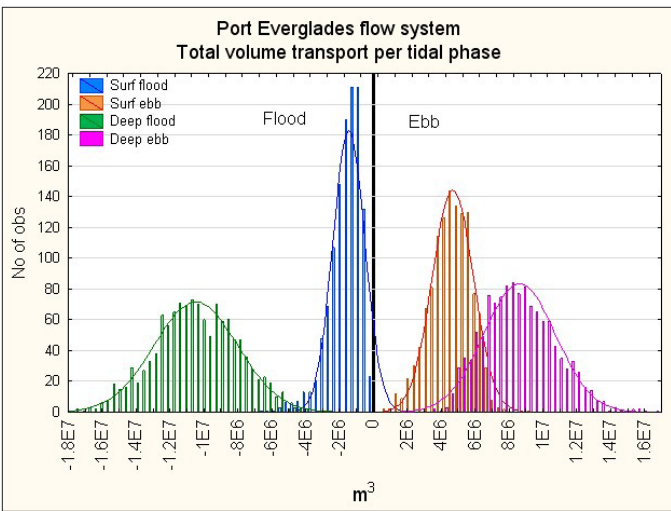

Figure 25. Histograms of the total volume transport for the surface and deep layers and for the flood and ebb tidal phases. These calculations were made using data from June 1, 2009 through May 31, 2011.
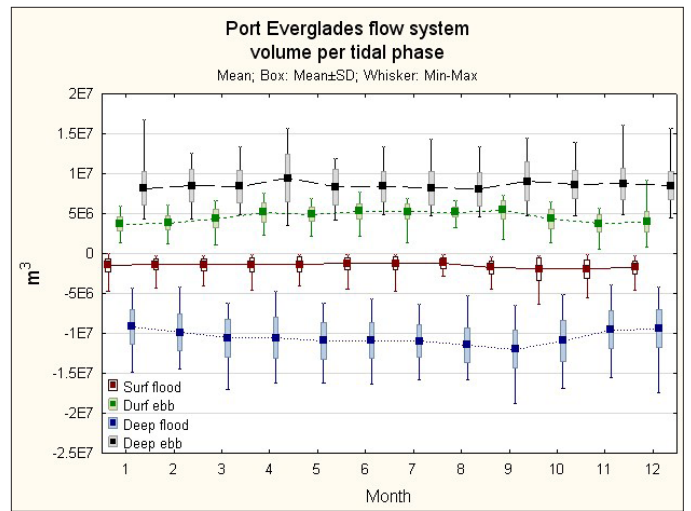

Figure 26. Volume per tidal phase grouped by month. Data are from June 1, 2009 through May 31, 2011.

Table 2. Period and volume transport per tidal phase. Data are from June 1, 2009 through May 31, 2011.

	Mean	Median	Lower Quartile	Upper Quartile	10%	90%	Standard Deviation
Surface flood period (hr)	4.18	4.2	3.6	4.8	2.9	5.3	1.1
Surface ebb period (hr)	8.14	8.2	7.7	8.7	7.0	9.1	1.5
Deep flood period (hr)	6.27	6.3	6.0	6.6	5.7	6.8	0.56
Deep ebb period (hr)	6.15	6.1	5.9	6.4	5.7	6.7	0.53
Surface flood volume ($m^3 \times 10^6$)	1.37	1.27	0.78	1.92	0.42	2.66	0.95
Surface ebb volume ($m^3 \times 10^6$)	4.41	4.43	3.57	5.32	2.73	6.00	1.41
Deep flood volume ($m^3 \times 10^6$)	10.15	10.27	8.34	11.91	6.67	13.45	2.62
Deep ebb volume ($m^3 \times 10^6$)	8.40	8.31	6.89	9.82	5.85	11.28	2.12

NOAA's National Weather Service were collected for the years 2009-2011, along with the climatic rainfall average (Figure 27). The monthly average rainfall at Ft. Lauderdale International Airport, along with the total volume transport in the surface ebb tide, are plotted in Figure 28. Some trends observed in the rainfall rate are also observed in the volume estimates. The linear correlation between these two data series is R = 0.59. Using a monthly average of rain rate to compare with the monthly volume transport through the inlet may be biased, however, as rainwater which is destined for the Port Everglades basin may be delayed by water management systems.

To illustrate a specific example of rainfall forcing of the inlet, the Q rates for the surface and deep layers, the water level above the instrument, and the daily precipitation rates from the Ft. Lauderdale International Airport for the period December 15-25, 2009 are plotted in Figure 29. On December 17, 2009, 16.8 cm of rainfall occurred, and on December 18, 2009, 6.2 cm of rainfall occurred. On December 18, 2009, the surface and deep ebb Qs began to increase in response to these rains. The ebb period in the surface layer was also seen to become longer with respect to the surface flood period.

4.10 Sources of Error

Data from the survey system showed that the channel flow could be quite variable in space and time. In particular, as the surface layer was being measured by the fixed system near the south side of the channel, inhomogeneities across the channel width could result in errors in the fixed system estimate of the surface layer. Data from the survey system

confirmed that these inhomogeneities did occur (Figure 15). Inspection of the surface layer data in Figure 11 showed significant variability in the velocity values measured by the system, especially at the peak ebb flow. This variability may be attributable to inhomogeneities similar to those observed in Figure 15. Visual observations of the channel south side made during data downloads indicated that the surface velocities varied from moment to moment. Inspection of Figures 10 and 19 showed that the general trend of the velocity data was captured by the system. Smoothing of the velocity data prior to the calculation of Q reduced the effects of the short-term variability.

The vertical division of the channel was based largely upon the CTD profile data. These data showed that, on the ebb

Table 3. Mean transport per tidal phase by month.

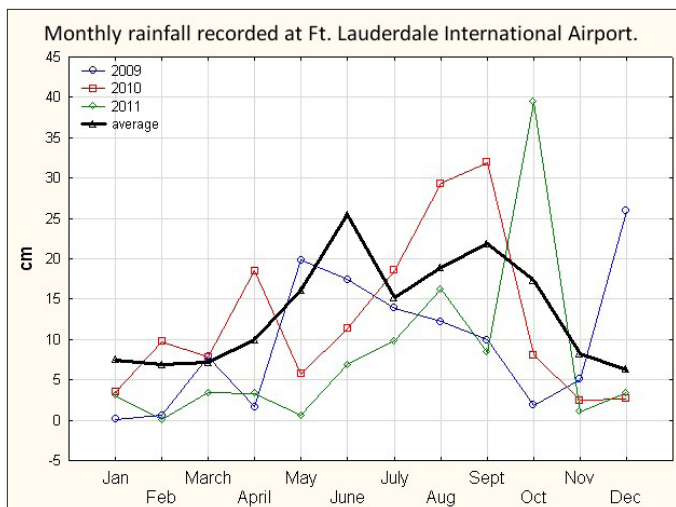| Month	Surface Ebb ($m^3 \times 10^6$)	Surface Flood ($m^3 \times 10^6$)	Deep Ebb ($m^3 \times 10^6$)	Deep Flood ($m^3 \times 10^6$)
Jan	3.703	1.464	8.177	9.177
Feb	3.827	1.400	8.519	9.884
Mar	4.374	1.408	8.388	10.567
Apr	5.149	1.403	9.438	12.546
May	4.883	1.391	8.347	10.925
Jun	5.318	1.241	8.389	10.878
Jul	5.269	1.260	8.226	10.960
Aug	5.157	1.203	8.078	11.472
Sep	5.477	1.729	9.001	11.977
Oct	4.359	1.949	8.642	10.929
Nov	3.786	1.916	8.723	9.525
Dec	3.989	1.728	8.492	9.402

Figure 27. Monthly rainfall for the years 2009-2011 and the average monthly rain rates at Ft. Lauderdale International Airport.

Figure 29. Example of a strong rain event with the surface and bottom Q from the H-ADCP system and the water level above the instrument.
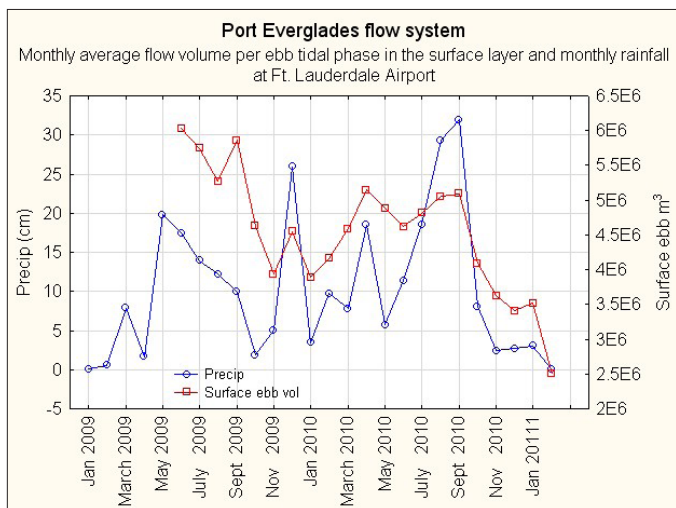

Figure 28. Monthly rainfall observed at Ft. Lauderdale International Airport and the monthly average surface ebb tide volume transport through the PESC.

5. Environmental Applications of Flow Data

5.1 Nutrient Fluxes

A group from Florida International University (FIU) was tasked with making nutrient samples in the channel while the flow measurement system was operative. Flow estimates for the surface and deep layers were provided to the FIU group and the fluxes of selected nutrients were generated. This is detailed in a separate report (Boyer *et al.*, 2013).

5.2 Fate of Materials Exiting the Port Everglades Channel

Ebb tide waters exiting the Port Everglades Inlet are dispersed into the nearby coastal environment. There is concern that, if these waters should contain substances deleterious to this environment and reach sensitive amenities in sufficient concentrations, harm might occur. In this section, we describe an effort to quantify the dispersion of substances exiting the channel. Figure 30 is an aerial photograph of a plume of material exiting the inlet. This plume was the result of dredging operations in the Intracoastal Waterway south of the inlet. An interesting aspect of this photograph is that the plume is heading south after exiting the inlet. The predominant current direction in this area is north; however, southern flow at nearshore locations occurs approximately 40-50% of the time (Carsey *et al.*, 2013).

tide, a layer of less dense/less saline water was often seen to form above the 3-m depth. Without the benefit of CTD data at each measurement interval, assigning an exact depth to the layer "break" was not possible. When the actual layer depth was other than this assigned depth, errors resulted in the estimation of flux through that layer.

Data collected with the survey system was used to calibrate the fixed system measurements. Performing the calibration transects was a difficult operation in Port Everglades, and there is no assurance that the survey system data are free from errors.
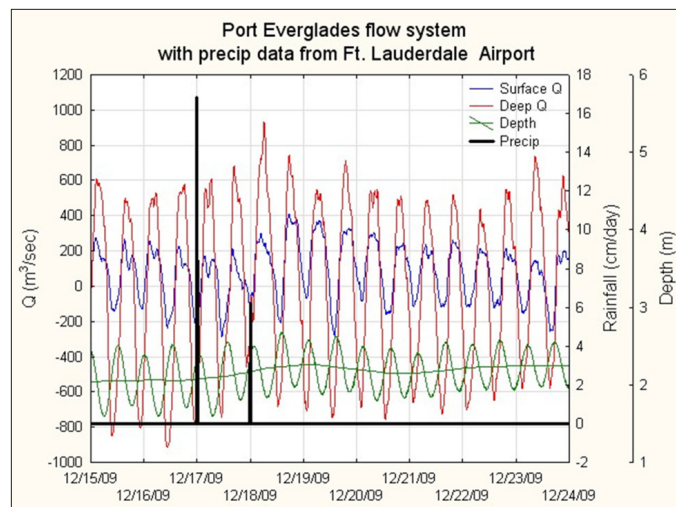
Figure 30. Port Everglades Inlet with a plume from dredging operations exiting the inlet on an ebb tide and dispersing to the south.

As part of the Florida Area Coastal Environment (FACE) program at AOML (http://www.aoml.noaa.gov/themes/ CoastalRegional/projects/FACE/faceweb.htm), a set of water samples was collected inside and just outside of the Port Everglades Channel (Figure 31). These samples were analyzed for nitrate plus nitrite (N+N), phosphate (P), silicate (Si), total suspended solids (TSS), and salinity.

To estimate the dilution of these substances after exiting the channel and entering the coastal ocean, the concentration of these substances at each sampling point was normalized by the value of that nutrient at station HW14. Station HW14 is located inside the PESC at the west end of the main channel, and concentrations of nutrients in samples collected at this point would be expected to be representative of the inland water that exits the PESC on the ebb tide. These normalized concentrations were then plotted, along with the absolute value of salinity, along lines in the east-west and north-south directions (Figure 32). The values of the normalized substances and salinity at station HW9 are also shown in the east-west plot and the offshore north-south plot. This was done as HW9 is far enough away from the inlet that values measured at this site would likely be more indicative of values observed in coastal ocean waters not affected by the inlet water.

This analysis was performed for data collected at the surface and at the mid-water depth. Figure 33 shows the normalized concentrations and salinity for the surface samples taken on
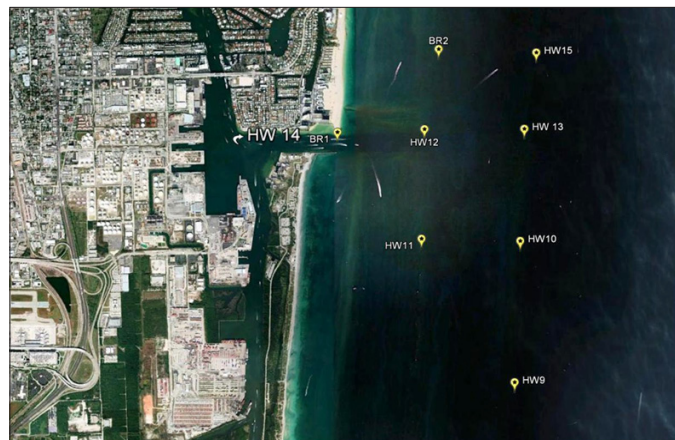

Figure 31. Port Everglades Inlet with FACE nutrient data sampling points identified.

The normalized sample data are plotted along three lines: east-west line (which also includes HW9 as a "background"); nearshore; and offshore north-south lines.

Figure 32. Port Everglades Inlet with FACE sampling stations and analysis lines.

September 29, 2011. From this we observed that along the east-west line the values of the normalized concentrations decreased, while the values of salinity increased. The values at HW13 in the east-west plot were near the values at HW9, suggesting that concentrations of the measured substances had essentially reached the background values. Figure 34 shows values taken at mid depths on September 29, 2011. Along the east-west line, values quickly approached the values seen at station HW9, suggesting that substances measured at the surface at HW14 did not advect downward to deeper depths. Figure 35 shows values taken at the surface on August 30, 2011. Similar to the surface plot from September 29, 2011 (Figure 33), the concentration of the substances fell rapidly at stations more distant from the inlet. Figure 36 shows mid-depth values taken on August 11, 2011. Similar to
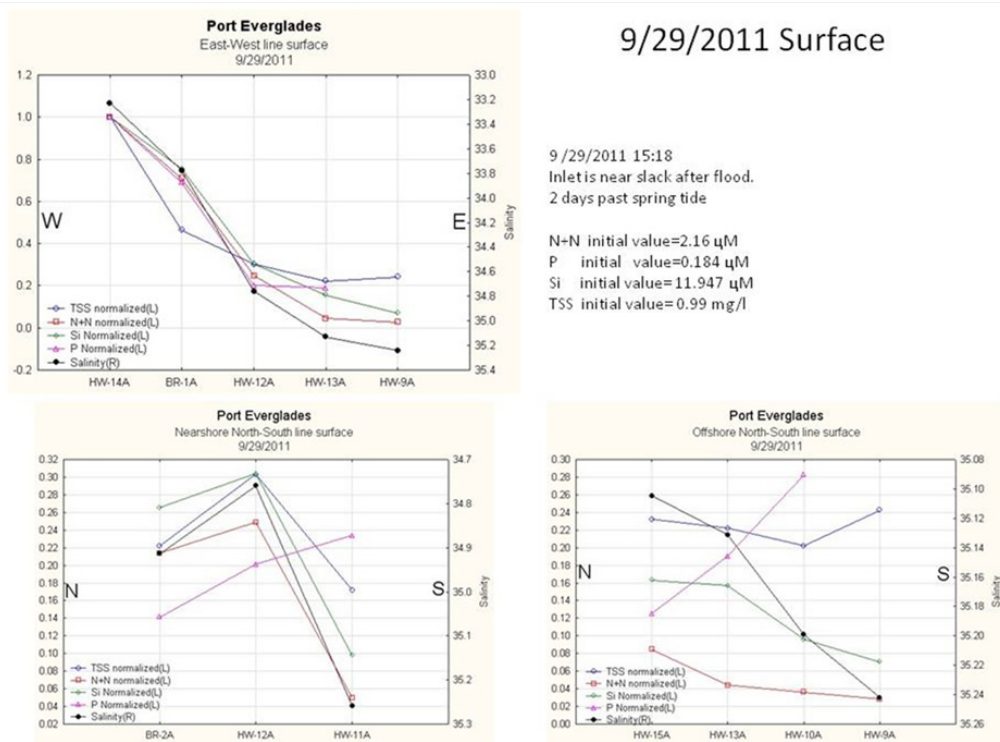
Figure 33. Analysis of relative concentrations and salinity at the surface on September 29, 2011.
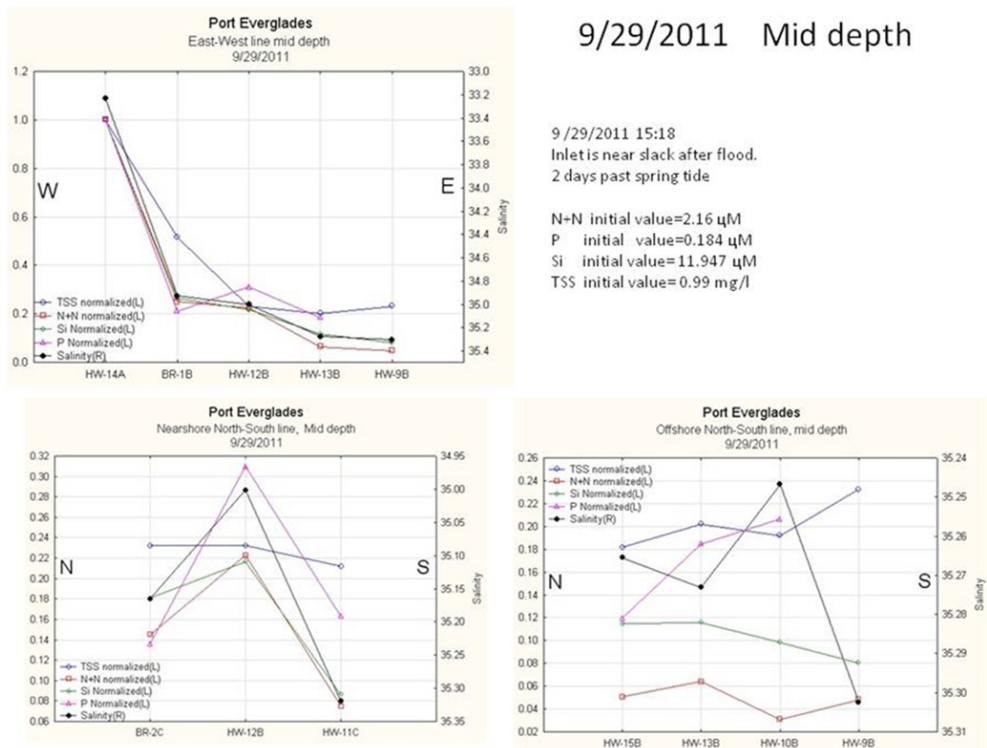

Figure 34. Analysis of relative concentrations and salinity at mid depths on September 29, 2011.
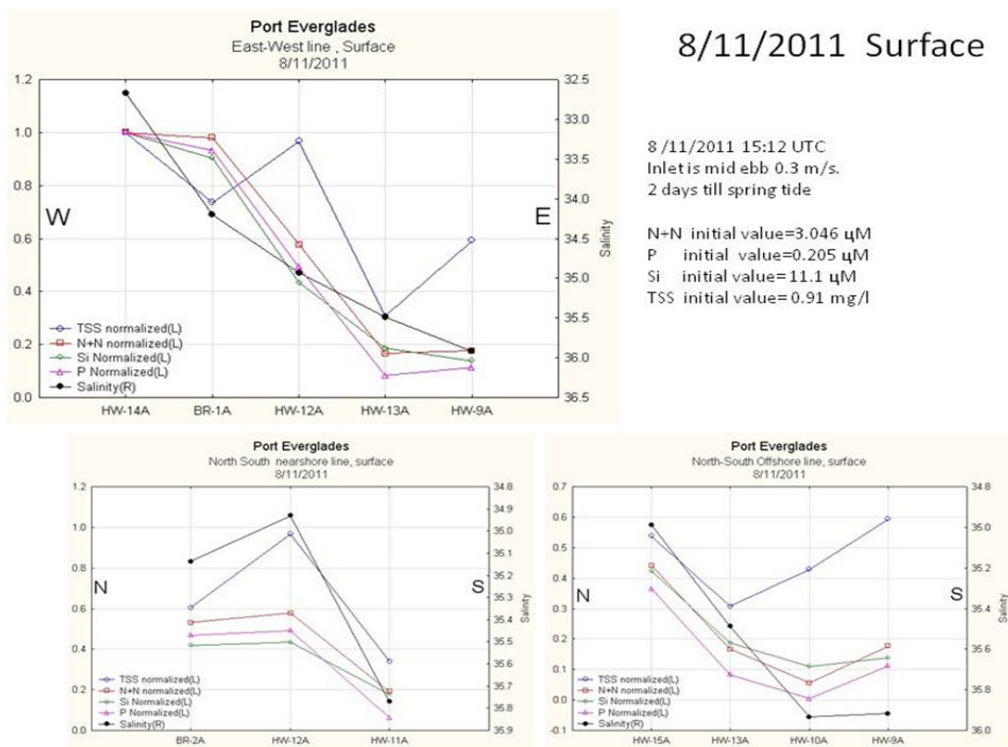
Figure 35. Analysis of relative concentrations and salinity at the surface on August 11, 2011.
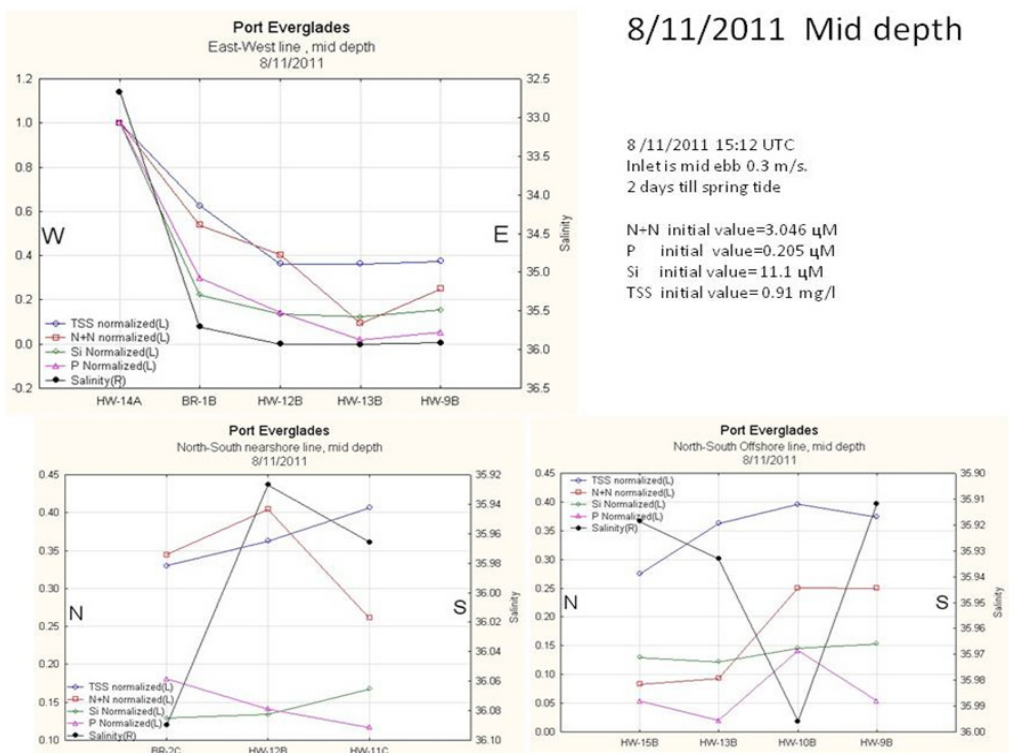

Figure 36. Analysis of relative concentrations and salinity at mid depths on August 11, 2011.
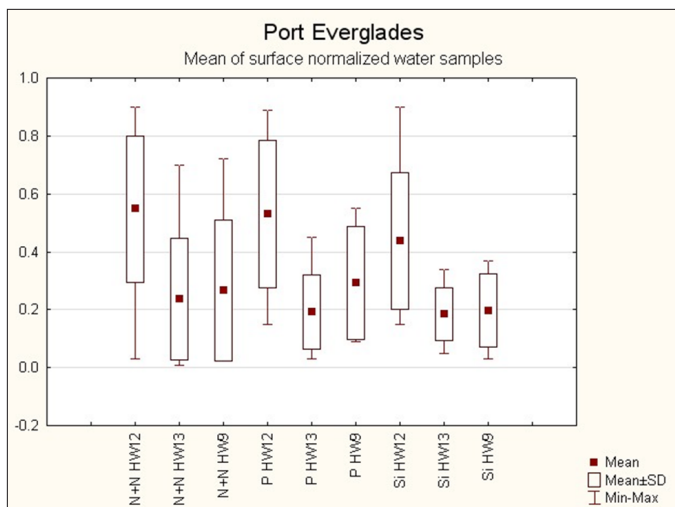
Figure 37. Box and whisker plot showing the mean, standard deviation, minimum, and maximum values of the normalized concentrations for N+N, P, and Si for stations HW2, HW3, and HW9.

the mid-depth plot from September 29, 2011 (Figure 34), the values at all stations except HW14 are near the same levels, suggesting that the substances observed in the HW14 sample did not advect downward to deeper depths.

Figure 37 is a summary of the values of the normalized concentrations of N+N, P, and Si for nine sets of surface data at stations HW2, HW3, and HW9. From Figures 30-37, several conclusions can be made:

- N+N, Si, and P appear to reside and dilute mostly in the surface layer.

- The surface values seen at HW13 (3.17 km from HW14) are close to those seen at HW9, implying that these nutrients have diluted to near background levels.

- If the levels at HW13 and HW9 are indicative of background levels, the levels at HW14 are typically five times higher than the background.

While these measurements consistently supported the above conclusions, they are a limited data set and may not represent all conditions observed at this site.

6. Summary

Data from a calibrated Doppler profiler was used to measure the vertical velocity structure in the Port Everglades Shipping Channel. The vertical structure of the channel was modeled as a two-layer system, and the flux rate and total transport per tidal cycle in those layers were estimated. The effects of rainfall on the the system were examined and the fate of materials exiting the channel into the coastal ocean was also examined.

7. References

Banks, K.W., B.M. Riegl, E.A. Shinn, W.E. Piller, and R.E. Dodge, 2007: Geomorphology of the southeast Florida continental reef tract (Miami-Dade, Broward, and Palm Beach counties, USA). *Coral Reefs,* 26:617-633.

Boyer, J.N. *et al.,* 2013: Report in preparation.

Carsey, T., S.J. Stamates, N. Amornthammarong, J.R. Bishop, F. Bloetscher, C.J. Brown, J.F. Craynock, S.R. Cummings, W.P. Dammann, J. Davis, C.M. Featherstone, C.J. Fisher, K.D. Goodwin, D.E. Meerhoff, J.R. Proni, C.D. Sinigalliano, P.K. Swart, and J.-Z. Zhang, 2012: Boynton Inlet 48-hour sampling intensives: June and September 2007. NOAA Technical Report, OAR-AOML-40, 43 pp.

Carsey, T., S.J. Stamates, J.R. Bishop, C.J. Brown, H.L. Casanova, C.M. Featherstone, M.L. Gidley, M. Kosenko, R.M. Kotkowski, C.D. Sinigalliano, L.A. Visser, and J.-Z. Zhang, 2013: Broward County coastal ocean: Water quality cruises, 2010-2012. NOAA Technical Report (in preparation).

Clay, C.S., and H. Medwin, 1977: *Acoustical Oceanography.* John Wiley and Sons, New York, 544 pp.

Huang, H., 2006: River discharge monitoring using horizontal acoustic Doppler current profiler (H-ADCP). Teledyne RD Instruments, Poway, CA, 25 pp. (available at http://www.rdinstruments.com/articles/River_discharge_monitoring_H-ADCP.pdf).

Levesque, V.A., and K.A. Oberg, 2012: Computing discharge using the index velocity method. U.S. Geological Survey Techniques and Methods 3-A23, 148 pp. (available at http://pubs.usgs.gov/tm/3a23/).

Ruhl, C.A., and M.R. Simpson, 2005: Computation of discharge using the index-velocity method in tidally-affected areas. U.S.Geological Survey, Scientific Investigations Report, 2005-5004, 31 pp.

Stamates, S.J., 2011: Using acoustic modeling to develop a hybrid H-ADCP configuration. *Proceedings, Tenth Current, Waves, and Turbulence Measurements Workshop,* Monterey, CA, March 20-23, 2011. Institute of Electrical and Electronic Engineers/Oceanic Engineering Society, 273-276.

Teledyne RD Instruments, 2006: *Acoustic Doppler Current Profiler Principles of Operation: A Practical Primer,* third edition, 56 pp.

U.S. Geological Survey, 2001: Kentucky mount II (available at http://hydroacoustics.usgs.gov/movingboat/pdfs/KYMount.pdf).